IMAGE ENHANCEMENT METHOD FOR UNDERWATER IMAGES BASED ON DISCRETE COSINE EIGENBASIS TRANSFORMATION

Tatsuya Baba, Keishu Nakamura, Seisuke Kyochi, and Masahiro Okuda

1: The University of Kitakyushu, Kitakyushu, Fukuoka, Japan
Email: s-kyochi@kitakyu-u.ac.jp, okuda-m@kitakyu-u.ac.jp

ABSTRACT

This paper proposes a novel image enhancement method for underwater images based on discrete cosine eigenbasis transformation (DCET). Since underwater images have a global strong dominant color, their colorfulness and contrast are often degraded. Typical color correction methods for natural images, i.e., computational color constancy, achromatize the colored illuminant of input images by dividing with an estimated illuminant color. However, this procedure produces unwanted color artifacts for underwater images. To solve this problem, we introduce a novel assumption that *achromatic illuminant images should have the DCT basis vectors as their principal component vectors*, which is termed as discrete cosine eigenbasis (DCE). According to the assumption, we achromatize underwater images by using a DCET that transforms the input image to the images having the DCE. By incorporating post image enhancement techniques, the proposed method provides sharper and brighter visual quality than conventional color correction and image enhancement methods.

Index Terms— Underwater images, Image enhancement, Computational color constancy, Discrete cosine transform

1. INTRODUCTION

It is a challenging task to remove a dominant color while keeping sharpness or brightness for various image processing tasks, e.g., image recognition. In the case of color correction for natural images, computational color constancy (CCC) [1] can efficiently correct the dominant color by estimating the color of the illuminant and multiplying their reciprocal to the input image. Unlike natural images, underwater images are more difficult to correct because they are dominated by a biased color of water such as blue or green, and their contrast tends to be very low. Thus, the direct application of the conventional CCC methods to underwater images cannot correct color appropriately or even produce unwanted color artifacts. Although Ancuti *et al.* perform a modified CCC method to an input image and synthesize it with color-contrast enhanced image [2], color artifacts remain in the resulting image. From another viewpoint, this color correction problem can be considered as the dehazing problem [3–5], where images are corrupted by global achromatic color artifact. He *et al.* proposed a single image dehezing method with *dark channel prior* (every minimum R, G, and B value in unhazed local regions should be close to 0) [3]. Thanks to the assumption, it removes the artifact satisfactory. Besides, there are several dehazing methods [4, 5] related to a prior. However, the dehazing methods for natural images result in poor visual quality for underwater images, since the chroma dominant color does not satisfy the priors assumption.

This work was supported in part by JSPS Grants-in-Aid(15K06076 and 17K14683).

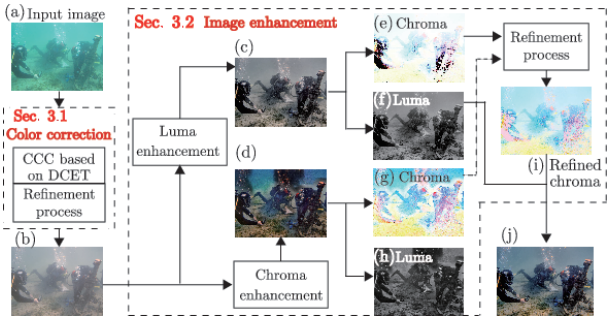

Fig. 1: Overview of our method.

We propose an image enhancement method of this problem. Our method consists of two steps; color correction and enhancement procedures as in Fig. 1. It is partially analogous to the conventional method of [2], but has a different procedure, specifically in color correction step. Our contributions of this paper are summarized as follows:

1. Unlike conventional CCC methods, we introduce a novel assumption that *achromatic illuminant images should have the DCT basis vectors as their principal component vectors*, which is termed as discrete cosine eigenbasis (DCE), and design a transformation matrix that can transform an input underwater image to the images having the DCE, which is termed as DCE transformation (DCET).
2. Thanks to the DCET, we obtain a less dominant color artifact image, but its contrast is low. As the second step, we create a luma enhanced and a chroma enhanced images in parallel and synthesize them, while the conventional method [3] uses only a color corrected image and a chroma contrast enhanced image.

The rest of this paper is organized as follows. Sec. 2 briefly reviews CCC methods and explains their difficulty for underwater image correction. Then, the proposed underwater image enhancement is explained in Sec. 3. The proposed algorithm is evaluated in the experiments in Sec. 4. Finally, this paper is concluded in Sec. 5.

Notations: Bold-faced lower-case and upper-case letters denote vectors and matrices, respectively. A set of N_r [row] and N_c [column] real-valued matrices is described as $\mathbb{R}^{N_r \times N_c}$. x_n and $X_{m,n}$ the n-th and (m,n)-th elements of a vector $\mathbf{x}$ and a matrix $\mathbf{X}$. $\mathrm{diag}(a_0, \ldots, a_{N-1})$ is the diagonal matrix of which diagonal entry $a_0, \ldots, a_{N-1}$. $\|\cdot\|_F$ is Frobenius norm. $E[\mathbf{x}]$ is the expectation operator of a random vector variable $\mathbf{x} \in \mathbb{R}^N$. We use the matrix

(a) White illuminant (b) Colored illuminant

(c) Distribution of (a) (d) Distribution of (b)

Fig. 2: Color distribution on white illuminant and color-illuminant image.

form $\mathbf{X} = \begin{bmatrix}\mathbf{r} & \mathbf{g} & \mathbf{b}\end{bmatrix}^\top \in \mathbb{R}^{3\times N}$ to represent color images with N pixels, where $\mathbf{r}$, $\mathbf{g}$, and $\mathbf{b} \in \mathbb{R}^N$ are R, G, and B channels, respectively. Moreover, the vector form $\mathbf{x}_i = \begin{bmatrix}r_i & g_i & b_i\end{bmatrix}^\top$ is used to represent R, G, and B of i-th pixel in a color image $\mathbf{X} \in \mathbb{R}^{3\times N}$.

2. PRELIMINARIES: CONVENTIONAL COMPUTATIONAL COLOR CONSTANCY

Unlike white illuminant images, such as Fig. 2(a), colored illuminant images are dominated by the color of the light source (Fig. 2(b)). To correct the colored illuminant image to a white illuminant image, CCC has been widely researched. It is generally accomplished by 1) estimating an illuminant color of the input image and 2) multiplying the reciprocal of the estimated color to the input image (it is called *diagonal model* in [1]). For example, Gray-World method [6] assumes that mean values of the R, G, and B channels $\boldsymbol{\mu} = [\mu_R,\ \mu_G,\ \mu_B]^\top$ of white illuminant images forms achromatic color, i.e., $\mu_R = \mu_G = \mu_B$, and estimates the illuminant color by $\boldsymbol{\mu}$. When the estimated illuminant color is $[\ell_R, \ell_G, \ell_B]^\top$ for an input image $\mathbf{X} = \begin{bmatrix}\mathbf{r}_x & \mathbf{g}_x & \mathbf{b}_x\end{bmatrix}^\top \in \mathbb{R}^{3\times N}$ with N pixels, a resulting CCC image $\mathbf{Z} \in \mathbb{R}^{3\times N}$ is given as:

$$\mathbf{Z} = \frac{\sqrt{\ell_R^2 + \ell_G^2 + \ell_B^2}}{\sqrt{3}} \mathrm{diag}\left(\frac{1}{\ell_R}, \frac{1}{\ell_G}, \frac{1}{\ell_B}\right)\mathbf{X}. \tag{1}$$

Although conventional computational color constancy efficiently works for natural images, it cannot work for underwater images because the estimated dominant color is significantly biased, e.g., $\ell_R \ll \ell_G,\ \ell_B$. In this case, some channel is over-emphasized in the resulting image as shown in Fig. 3(b).

3. PROPOSED UNDERWATER IMAGE ENHANCEMENT

3.1. Color Correction for Underwater Images

As shown in Sec. 2, the diagonal model cannot correct efficiently for underwater images. Thus, we introduce another approach based on a novel assumption. As shown in Fig. 2(c), many of color samples of white illuminant images tends to gather along the direction $\frac{1}{\sqrt{3}}\begin{bmatrix}1 & 1 & 1\end{bmatrix}^\top$. According to this characteristic, we introduce the following assumption.

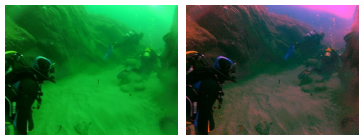

(a) Input (b) Gray world

(c) Prop. (Grobal) (d) Prop. (Line) (e) Prop. (Refine.)

Fig. 3: Color correction on underwater images.

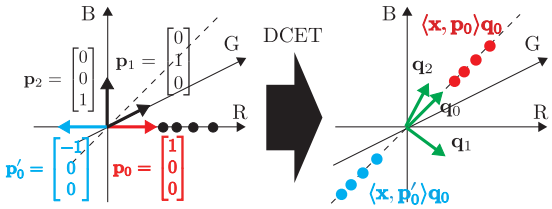

Fig. 4: Sign determination of $\mathbf{D}$.

Assumption 1. *After some color correction processing, eigenvectors of the covariance matrix or the correlation matrix obtained from the resulting image should form the discrete cosine basis:*

$$\mathbf{Q} = \begin{bmatrix}\mathbf{q}_0 & \mathbf{q}_1 & \mathbf{q}_2\end{bmatrix} = \begin{bmatrix}\frac{1}{\sqrt{3}} & \frac{1}{\sqrt{2}} & \frac{1}{\sqrt{6}} \\ \frac{1}{\sqrt{3}} & 0 & -\frac{2}{\sqrt{6}} \\ \frac{1}{\sqrt{3}} & -\frac{1}{\sqrt{2}} & \frac{1}{\sqrt{6}}\end{bmatrix}. \tag{2}$$

We call the set of eigenvectors of the covariance or correlation matrix as eigenbasis, and in particular, when eigenbasis forms discrete cosine basis, we term it as DCE in this paper.

With this assumption in mind, we design a transformation matrix $\mathbf{K} \in \mathbb{R}^{3\times 3}$ such that, for an N-sample input image $\mathbf{X} \in \mathbb{R}^{3\times N}$, the transformed image $\mathbf{Z} = \mathbf{K}\mathbf{X}$ has the DCE, which $\mathbf{K}$ is called DCE transformation (DCET).

3.1.1. Design of DCET Matrix

This section clarifies the design procedure of the DCET matrix. For simple discussion, we consider the correlation matrix $E[\mathbf{z}\mathbf{z}^\top] \in \mathbb{R}^{3\times 3}$, not the covariance matrix, where $\mathbf{z} \in \mathbb{R}^3$ denotes the random vector variable for the RGB sample of the transformed image. The correlation matrix of the transformed image should be diagonalized by the DCE $\mathbf{Q}$ in (2) as:

$$E[\mathbf{z}\mathbf{z}^\top] = \mathbf{Q}\mathbf{D}_z\mathbf{Q}^\top, \tag{3}$$

where $\mathbf{D}_z = \mathrm{diag}(\alpha_z\ \beta_z, \gamma_z) \in \mathbb{R}^{3\times 3}$ is the matrix containing the eigenvalues. On the other hand, from $\mathbf{z} = \mathbf{K}\mathbf{x}$ ($\mathbf{x} \in \mathbb{R}^3$ is the random vector variable for the RGB sample of the input image), we can derive that

$$E[\mathbf{z}\mathbf{z}^\top] = \mathbf{K}E[\mathbf{x}\mathbf{x}^\top]\mathbf{K}^\top = \mathbf{K}\mathbf{P}\mathbf{D}_x\mathbf{P}^\top\mathbf{K}^\top, \tag{4}$$

where $\mathbf{P} = \begin{bmatrix}\mathbf{p}_0 & \mathbf{p}_1 & \mathbf{p}_2\end{bmatrix} \in \mathbb{R}^{3\times 3}$ and $\mathbf{D}_x = \mathrm{diag}(\alpha_x,\ \beta_x, \gamma_x) \in \mathbb{R}^{3\times 3}$ are the eigenbasis and the eigenvalues of an input image. By

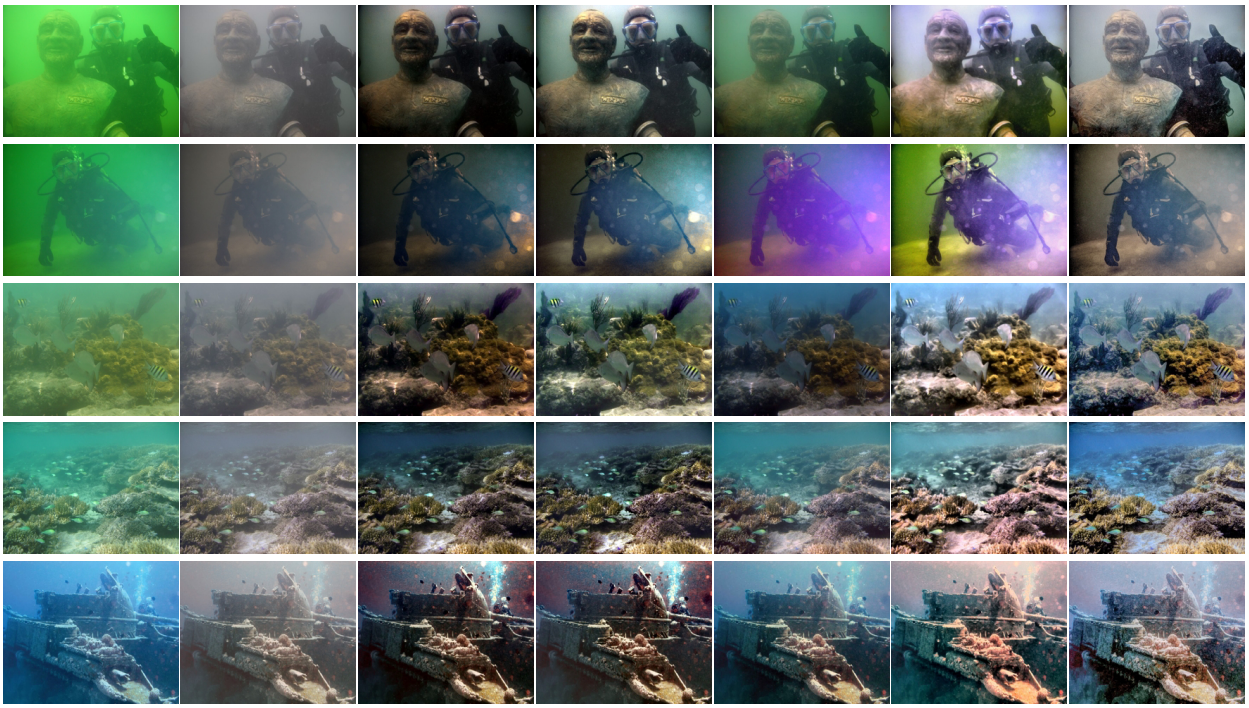

(a) Input (b) Our CCC (c) Our CCC w/ [3] (d) Our CCC w/ [5] (e) [7] (f) [2] (g) Our result

Fig. 5: Comparison with conventional methods.

introducing $\mathbf{D} = \mathrm{diag}\left(\pm\sqrt{\frac{\alpha_z}{\alpha_x}}, \pm\sqrt{\frac{\beta_z}{\beta_x}}, \pm\sqrt{\frac{\gamma_z}{\gamma_x}}\right)$, from (3) and (4), we can reduce that:

$$\mathbf{Q}\mathbf{D}_z\mathbf{Q}^\top = \mathbf{Q}\mathbf{D}\mathbf{D}_x\mathbf{D}\mathbf{Q}^\top = \mathbf{K}\mathbf{P}\mathbf{D}_x\mathbf{P}^\top\mathbf{K}^\top. \tag{5}$$

Finally, the DCET matrix $\mathbf{K}$ can be given as $\mathbf{K} = \mathbf{Q}\mathbf{D}\mathbf{P}^\top$.

Next, we discuss how to determine the diagonal matrix $\mathbf{D}$. For every input color $\mathbf{x} \in \mathbb{R}^3$, the transformed color $\mathbf{y} = \mathbf{K}\mathbf{x}$ can be expressed as the linear combination of $\{\mathbf{q}_i\}$ as:

$$\mathbf{y} = D_{0,0}\langle\mathbf{p}_0, \mathbf{x}\rangle\mathbf{q}_0 + D_{1,1}\langle\mathbf{p}_1, \mathbf{x}\rangle\mathbf{q}_1 + D_{2,2}\langle\mathbf{p}_2, \mathbf{x}\rangle\mathbf{q}_2. \tag{6}$$

Since our purpose is just to rotate the color distribution of an input image so that the eigenbasis of the rotated image forms equal to the discrete cosine basis, there is no need to stretch the distribution. Thus, we simply set the absolute value of its diagonal element as 1, i.e., $|D_{i,i}| = 1$. Their signs should be determined in the following way. Every vector $\mathbf{p}_i$ is not necessarily directed to the same quadrant. In Fig. 4, $\mathbf{P} = \begin{bmatrix}\mathbf{p}_0 & \mathbf{p}_1 & \mathbf{p}_2\end{bmatrix}$ converts the input colors (the black circles on the R axis in the left figure) appropriately (the red circles in the right figure) and $\mathbf{P}' = \begin{bmatrix}\mathbf{p}'_0 & \mathbf{p}_1 & \mathbf{p}_2\end{bmatrix}$ does not (blue circles in the negative domain in the right figure). In order to modify such cases, it is enough to determine $\mathbf{D}$ as $D_{i,i} = \mathrm{sign}(\langle\mathbf{p}_i, \mathbf{q}_i\rangle)$.

3.1.2. *Detail Algorithm of DCET*

There would be several ways to design and apply the DCET matrix $\mathbf{K}$. The simplest one is to construct $\mathbf{P}$ via eigenvalue decomposition as $\frac{1}{N}\mathbf{X}\mathbf{X}^\top = \mathbf{P}\mathbf{\Gamma}\mathbf{P}^\top$, for whole input image $\mathbf{X} \in \mathbb{R}^{3\times N}$, determine $\mathbf{D}$ as in Sec. 3.1.1, and apply $\mathbf{K}\mathbf{X} = \mathbf{Q}\mathbf{D}\mathbf{P}^\top\mathbf{X}$ (we denote it as an global approach). However, this produces unwanted color artifacts, as in Fig. 3(c).

To reduce the artifacts, we take a line-by-line approach as follows. For an $M \times N$ input image, we extract each column $\mathbf{X}_i^{(c)} \in \mathbb{R}^{3\times M}$, $(i = 0, \ldots, N-1)$ and construct $\mathbf{K}_i^{(c)} = \mathbf{Q}\mathbf{D}_i^{(c)}(\mathbf{P}_i^{(c)})^\top$, where $\frac{1}{N}\mathbf{X}_i^{(c)}(\mathbf{X}_i^{(c)})^\top = \mathbf{P}_i^{(c)}\mathbf{\Gamma}_i^{(c)}(\mathbf{P}_i^{(c)})^\top$, and apply $\mathbf{K}_i^{(c)}\mathbf{X}_i^{(c)}$. Then, the vertically color-corrected image $\mathbf{X}^{(c)}$ can be obtained. This procedure is also performed for each row of the input image, and one obtains the horizontally color-corrected image $\mathbf{X}^{(r)}$. Finally, $\mathbf{X}^{(c)}$ and $\mathbf{X}^{(r)}$ are integrated simply by taking the average of the two images.

$$\widehat{\mathbf{X}} = \frac{1}{2}\left(\mathbf{X}^{(c)} + \mathbf{X}^{(r)}\right). \tag{7}$$

As shown in Fig. 3(d), the line-by-line DCET can reduce the color artifacts better than the global one.

3.1.3. *Refinement Process*

We do not use $\widehat{\mathbf{X}}$ in (7) itself since it still has line artifacts generated by the DCET along the rows and columns. Thus, we approximate the color of $\widehat{\mathbf{X}}$ from the input image by using the well-known quadratic color transformation[1] [8]. Specifically, we finds the transformation matrix $\mathbf{T}^\star \in \mathbb{R}^{3\times 10}$ as:

$$\mathbf{T}^\star = \underset{\mathbf{T}\in\mathbb{R}^{3\times 10}}{\arg\min} \|\mathbf{T}\mathbf{X}' - \widehat{\mathbf{X}}\|_F^2 + \epsilon\|\mathbf{T}\|_F^2, \tag{8}$$

[1]This transformation is useful when one wants to approximate from some noise-free blurred image to a noisy sharp image, in order to generate a noise-free sharp image.

where $\mathbf{X}' \in \mathbb{R}^{10\times N}$ is a matrix composed of each pixel in $\mathbf{X}$, $\mathbf{X}' = [\mathbf{x}'_0, \ldots, \mathbf{x}'_{N-1}]$, $\mathbf{x}'_i = [r_i^2, g_i^2, b_i^2, r_i g_i, r_i b_i, g_i b_i, r_i, g_i, b_i, 1]^\top$, r_i, g_i, and b_i denote the R, G, and B color channel of the i-th pixel $\mathbf{x}_i$, respectively. ϵ is a weight parameter of Thikhonov regularization. Using the estimated matrix $\mathbf{T}^\star$, the final color-corrected image $\mathbf{X}^{cc} \in \mathbb{R}^{3\times N}$ is calculated as $\mathbf{X}^{cc} = \mathbf{T}^\star \mathbf{X}'$. This procedure further reduces the artifacts, as in Fig. 3(e).

3.2. Image enhancement

After the DCET, a hazy image can be obtained. Therefore, we apply the dehazing-like technique to the color corrected image to enhance the visual quality. In this work, we introduce not only a chroma enhanced image but also a luma contrast enhanced one, and then synthesize them to a final image, whereas Ancuti *et al.* only fuses the color corrected image with the diagonal model and chroma enhanced one [2]. In the following, we explain the detail procedure.

3.2.1. Luma Contrast Enhancement

We apply the technique proposed in [9] to the color-corrected image $\mathbf{X}^{cc}$ to obtain the luma contrast enhanced image $\mathbf{Z}_1 \in \mathbb{R}^{3\times N}$. Briefly speaking, 1) it decomposes each R, G, and B channel by Laplacian Pyramid, 2) performs a tone-mapping operator that enhances the detail, and 3) reconstructs the enhanced image from the pyramid (for more information, see [9]).

3.2.2. Chroma Contranst Enhancement

Since the chroma contrast remarkably decreases in the underwater images, the chroma enhancement is performed in each local region as follows. The operator that extracts an $L \times L$ square local region Ω_i centered on a pixel i is defined as $P_i(\cdot)$, and chroma contrast enhancement of the R channel in a target local region is expressed as

$$r_{i,j}^{ce} = \frac{r_j^{cc} - \min(P_i(\mathbf{X}^{cc}))}{\max(P_i(\mathbf{X}^{cc})) - \min(P_i(\mathbf{X}^{cc}))} \max(P_i(\mathbf{X}^{cc})), \quad \forall j \in \Omega_i. \tag{9}$$

Since, after applying (9), the multiple contrast enhanced values are assigned at i-th pixel, i.e. $\{r_{i-1,i}^{ce}, r_{i,i}^{ce}, r_{i+1,i}^{ce}, \cdots\}$, the values should be averaged. The result $\mathbf{r}^{ce} \in \mathbb{R}^N$ is expressed as:

$$r_i^{ce} = \frac{1}{L^2} \sum_{k\in\mathcal{N}(i)} r_{k,i}^{ce}, \ \mathcal{N}(i) = \{k \in \mathbb{N} \mid i \in \Omega_k\}. \tag{10}$$

Performing to the G and B channel in the same way, the chroma contrast enhanced image $\mathbf{Z}_2 = \begin{bmatrix}\mathbf{r}^{ce} & \mathbf{g}^{ce} & \mathbf{b}^{ce}\end{bmatrix}^\top$ is obtained.

3.2.3. Chroma Refinement

In Sec. 3.2.1 and Sec. 3.2.2, we have two contrast enhanced images that characteristic is summarized as

- The luma of $\mathbf{Z}_1 = \begin{bmatrix}\mathbf{r}_1 & \mathbf{g}_1 & \mathbf{b}_1\end{bmatrix}^\top$ obtained by the luma contrast enhancement (Sec. 3.2.1) has sharp detail, but its chroma is not bright.
- The luma of $\mathbf{Z}_2 = \begin{bmatrix}\mathbf{r}_2 & \mathbf{g}_2 & \mathbf{b}_2\end{bmatrix}^\top$ obtained by the chroma contrast enhancement (Sec. 3.2.2) has unsharp detail, but its chroma is bright.

To take the advantages of the two images, first, we decompose each image $\mathbf{Z}_k$ into luminace and chrominance $\mathbf{y}_k \in \mathbb{R}^N$ and $\mathbf{C}_k = \begin{bmatrix}\widetilde{\mathbf{r}}_k & \widetilde{\mathbf{g}}_k & \widetilde{\mathbf{b}}_k\end{bmatrix}^\top \in \mathbb{R}^{3\times N}$ ($k = 1$ or 2) as:

$$y_{k,i} = \frac{r_{k,i}}{s_{k,i}} r_{k,i} + \frac{g_{k,i}}{s_{k,i}} g_{k,i} + \frac{b_{k,i}}{s_{k,i}} b_{k,i}, \quad \mathbf{c}_{k,i} = \frac{\mathbf{z}_{k,i}}{y_{k,i}}, \tag{11}$$

where $r_{k,i}$, $g_{k,i}$, $b_{k,i}$ are the value of red, green and blue at the i-th pixel of $\mathbf{Z}_k$, and $s_{k,i} = r_{k,i} + g_{k,i} + b_{k,i}$.

The less bright chrominance $\mathbf{C}_1$ is approximated to the bright chrominance $\mathbf{C}_2$ by performing the quadratic optimization according to (8). The color conversion matrix $\mathbf{T}^{c\star}$ is given as

$$\mathbf{T}^{c\star} = \arg\min_{\mathbf{T}^c} \|\mathbf{T}^c {\mathbf{C}_1}' - \mathbf{C}_2\|_F^2 + \epsilon \|\mathbf{T}_c\|_F^2, \tag{12}$$

where ${\mathbf{C}_1}' \in \mathbb{R}^{10\times N}$ is a matrix obtained by extending each pixel value as in (8). Using the sharp luminance $\mathbf{y}_1$ and the bright chrominance $\mathbf{C}^\star = \mathbf{T}^{c\star} {\mathbf{C}_1}'$, each pixel value of the final processing result image $\mathbf{Z}^\star \in \mathbb{R}^{3\times N}$ is given as $\mathbf{z}_i^\star = y_{1,i}\, \mathbf{c}_i^\star$.

The input image, the color-corrected image, the luma and chroma enhanced results, and the final enhanced image are shown in Fig. 1. As an effect of the image integration process, the final output result (j) has the high contrast of the contrast-enhanced image (f) and the vivid color of the color-enhanced image (i).

4. EXPERIMENTS

We show the effectiveness of our method by comparing our image enhancement results for underwater images with conventional methods. As the conventional underwater enhancement methods, we use [2, 7]. Since the result image after our CCC in Sec. 3.1 is similar to a hazy image, we also evaluate the dehazing methods [3, 5] with our CCC. The parameter for Tikhonov regularization ϵ used in (8) and (12) is set to 1×10^{-5}, and the local region Ω_i in Sec. 3.2.2 is set to 31×31. All of the experiment images were obtained from Ancuti's web page [2].

4.1. Comparison with conventional methods

Fig. 5 shows the results of our and conventional methods. Since the dehazing methods [3, 5] after our CCC (Figs. 5(c) and (d)) can remove haze and emphasize its contrast, but some parts are blurred in dark regions. On the other hand, the methods [2, 7] can almost remove the color of water (Figs. 5(e) and (f)), and it has colorful results. However, one can see in the top two results, color correction effect is inadequate. In our method, the object color in the image is vivid and has high contrast (Fig. 5(g)).

We discuss the processing time of the proposed method. In this method, the whole algorithm is implemented by MATLAB, and the total processing time using a computer of 3.20 GHz Core i 5 CPU for an image 1080×1920 is about 7 seconds. In each processing, the color correction is about 1.5 seconds, the luma contrast enhancement processing is about 3.6 seconds, the chroma contrast enhancement processing is about 0.7 second, and the integration processing is 0.7 second.

5. CONCLUDING REMARKS

This paper proposed the color correction and image enhancement method for underwater images. Based on the new assumption, we introduced the DCET in the CCC procedure, which enables us to robustly correct the dominant color of underwater images. In the image enhancement, a chroma contrast enhancement image and a luma contrast enhancement image are generated, and an image having a vivid color and sharp detail is generated through the integration. The experiments showed the effectiveness of the proposed method by comparing with the conventional methods.

6. REFERENCES

[1] A. Gijsenij, T. Gevers, and J. van de Weijer, "Computational color constancy: Survey and experiments," *IEEE Trans. Image Process.*, vol. 20, no. 9, pp. 2475–2489, Sep. 2011.

[2] C. Ancuti, C. O. Ancuti, T. Haber, and P. Bekaert, "Enhancing underwater images and videos by fusion," in *Proc. IEEE Conf. CVPR*, June 2012, pp. 81–88.

[3] K. He, J. Sun, and X. Tang, "Single image haze removal using dark channel prior," *IEEE T. PAMI*, vol. 33, no. 12, pp. 2341–2353, Dec 2011.

[4] Raanan Fattal, "Dehazing using color-lines," *ACM T. Graph. (Proc. SIGGRAPH)*, vol. 34, no. 1, pp. 13:1–13:14, Dec. 2014.

[5] D. Berman, T. Treibitz, and S. Avidan, "Non-local image dehazing," in *Proc. IEEE Conf. CVPR*. IEEE, 2016.

[6] Marc Ebner, *Color Constancy*, Wiley Publishing, 1st edition, 2007.

[7] K. Iqbal, S. R. Adbul, M. Osman, and A. Z. Talib, "Underwater image enhancement using an integrated colour model," in *Int. J. Comput. Sci.*, 2007, vol. 32, pp. 239–244.

[8] Baoyuan Wang, Yizhou Yu, and Ying-Qing Xu, "Example-based image color and tone style enhancement," in *ACM SIGGRAPH 2011 Papers*, New York, NY, USA, 2011, SIGGRAPH '11, pp. 64:1–64:12, ACM.

[9] T. Jinno, H. Watanabe, and M. Okuda, "High contrast tone-mapping and its application for two-layer high dynamic range coding," in *Signal Information Processing Association Annual Summit and Conference (APSIPA ASC), 2012 Asia-Pacific*, Dec 2012, pp. 1–4.